Journal of Orthopaedic Surgery and Research

RESEARCH ARTICLE

Open Access

Biomechanical characteristics of ligament injuries in the knee joint during impact in the upright position: a finite element analysis

Jia Li[1,2], Hanbing Liu[1,2], Mingyao Song[1], Fei Lin[1], Ziya Zhao[1,2], Zhenghui Wang[1], Liming Hou[1,2*], Guoan Zhao[1*] and Wu Ren[1,2*]

Abstract

Background Our study aims to examine stress–strain data of the four major knee ligaments—the anterior cruciate ligament (ACL), the posterior cruciate ligament (PCL), the medial collateral ligament (MCL), and the lateral collateral ligament (LCL)—under transient impacts in various knee joint regions and directions within the static standing position of the human body. Subsequently, we will analyze the varying biomechanical properties of knee ligaments under distinct loading conditions.

Methods A 3D simulation model of the human knee joint including bone, meniscus, articular cartilage, ligaments, and other tissues, was reconstructed from MRI images. A vertical load of 300 N was applied to the femur model's top surface to mimic the static standing position, and a 134 N load was applied to the impacted area of the knee joint. Nine scenarios were created to examine the effects of anterior, posterior, and lateral external forces on the upper, middle, and lower regions of the knee joint.

Results The PCL exhibited the highest stress levels among the four ligaments when anterior loads were applied to the upper, middle, and lower parts of the knee, with maximum stresses at the PCL-fibula junction measuring 59.895 MPa, 27.481 MPa, and 28.607 MPa, respectively. Highest stresses on the PCL were observed under posterior loads on the upper, middle, and lower knee areas, with peak stresses of 57.421 MPa, 38.147 MPa, and 26.904 MPa, focusing notably on the PCL-tibia junction. When a lateral load was placed on the upper knee joint, the ACL showed the highest stress 32.102 MPa. Likewise, in a lateral impact on the middle knee joint, the ACL also had the highest stress of 29.544 MPa, with peak force at the ACL-tibia junction each time. In a lateral impact on the lower knee area, the LCL had the highest stress of 22.279 MPa, with the highest force at the LCL-fibula junction. Furthermore, the maximum stress data table indicates that stresses in the ligaments are typically higher when the upper portion of the knee is affected compared to when the middle and lower parts are impacted.

Conclusions This study recommends people avoid impacting the upper knee and use the middle and lower parts of the knee effectively against external forces to minimize ligament damage and safeguard the knee.

Keywords Human knee joint, Ligament, Finite element model, Biomechanical analysis, Stress

*Correspondence:
Liming Hou
780178657@qq.com
Guoan Zhao
guoanzhao@xxmu.edu.cn
Wu Ren
renwu88@126.com
Full list of author information is available at the end of the article

Introduction

The knee joint is one of the seven major joints in the human body. It consists of the distal femur, proximal tibia, patella, meniscus, femoral cartilage, and tibial plateau cartilage, all of which are interconnected by ligaments and tendons [1]. As the largest and most complex joint in the human body, it plays a pivotal role in human mobility. Due to its anatomical features and physiological load-bearing capacity, it is highly susceptible to injury. Especially in confrontational sports like wrestling and taekwondo, involving physical contact and forceful leg movements, the high intensity and confrontations frequently lead to injuries among athletes. Some surveys have shown that the mild to moderate injuries that athletes often experience include patellar strain and knee joint sprains [2], while severe injuries include meniscus injuries and ligament tears. Notably, ligament injuries account for a significant proportion, with a rate as high as 23.6% [3].

The ligaments in the knee include the patellar ligament (PL), anterior cruciate ligament (ACL), posterior cruciate ligament (PCL), medial collateral ligament (MCL) and lateral collateral ligament (LCL). They consist of dense connective tissue that is used to enhance and maintain joint stability during movement, as well as limit motion beyond the physiological range. The cruciate ligaments restrict the knee joint's anterior and posterior movement, while the medial and lateral collateral ligaments constrain its lateral motion (Fig. 1).

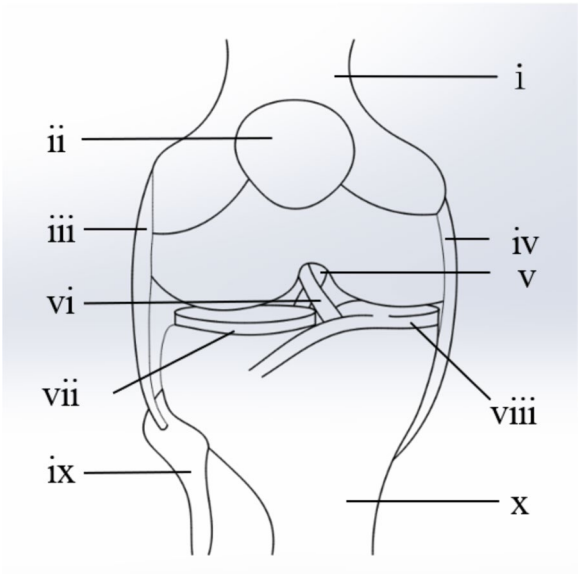

Fig. 1 Schematic diagram of the anatomical structure of the knee joint with (i) Femur, and (ii) Patella. (iii) LCL. (iv) MCL. (v) PCL. (vi) ACL. (vii) Lateral meniscus. (viii) Medial meniscus. (ix) Fibula. (x) Tibia

In recent years, with the rapid advancement of image processing, computer technology, and medical image modeling, finite element analysis (FEA) has seen significant development in knee joint mechanics simulation experiments. Currently, numerous domestic and international researchers utilize reverse modeling tools (e.g., Mimics, Geomagic, etc.) and FEA tools (e.g., ANSYS, COMSOL, ABAQUS, etc.) using MRI images to create knee joint models and perform analyses, replicating varying levels of biomechanical processes [4, 5]. Although FEA can provide convenience for knee joint hard and soft tissue related research, there is a certain degree of difficulty in the modeling operation in the software. Therefore, a study [6] has described the operation of the software tools and precautions in detail, to provide help for subsequent optimization of model simulation, analysis and design, deeper finite element numerical computation, and close integration of simulation technology.

In numerous finite element studies of the knee joint, scholars have primarily focused on bone and cartilage injuries due to the simplicity of the bone structure, stability of material properties, and clarity of boundary conditions and load constraints [7–9]. The results of their study show that a distinct impact of the tibia or meniscus, varus/valgus deformity of femur had an obvious effect on the contact area and stress distribution of knee joint. Among them, the 3D finite element model developed by Donahue [10] and his colleges includes bone, ligaments, meniscus, and cartilage. This study specifically examined the meniscus and cartilage to assess how bone deformation impacts joint contact behavior. The proximal tibiofibular joint (PTFJ) is easily ignored, although many diseases of the knee are caused by PTFJ injuries. Therefore, Shao [11] conducted a comparative study on the biomechanical mechanisms of the knee joint in normal and PTFJ-injured states, analyzing and exploring the role of PTFJ in maintaining posterior-lateral stability of the knee joint. Furthermore, Numan [12] created 3D SolidWorks model files to evaluate the optimal treatment for tibiofibular joint injuries. The intact model, injury model, and 8 different fixation models were created that 3.5 mm screw and suture-button were used in. The models were compared in terms of lateral fibular translation, posterior fibular translation and external rotation of fibula compared of tibia and stress values occurred on screws and suture-buttons.

Performing finite element studies in soft tissues is more challenging than in bony structures due to their intricate geometry, nonlinearity, and significant deformation rates. This necessitates the use of more sophisticated material models and boundary conditions to accurately capture their behavior. Moreover, this category of research is limited by a lack of soft tissue experimental data, hindering the validation and calibration of the model. Several

scholars have concentrated on studying knee ligaments [13–16]. The 3D knee model of their study offers a detailed view of the ACL and patellofemoral ligament (PFL), allowing assessment of ligament stress distribution and joint contact pressures in various loading scenarios, thus guiding suggestions for ligament reconstruction surgery. Li [17] and his team transcended the limitations of earlier models that only verified the efficacy of ligaments or cartilage individually, improving the practicality and universality of the model. Furthermore, Peña [18] developed a detailed 3D finite element model of the healthy human knee, focusing on examining the collective functions of ligaments and menisci in load distribution and knee stability. This study by Yang and his team [19] aimed to analyze the stress and strain changes of the ACL at different knee flexion angles using a 3D finite element model. The magnitude and concentration area of stress and strain of ACL at knee flexion angles 0°, 30°, 60° and 90° were assessed.

In the finite element studies of knee joint ligaments, most research [20–23] has focused on just one or two ligaments, they individually explored the stresses and strains of MCL, ACL, and single-bundle PCL under different loads and boundary conditions. This is because it is challenging to replicate the intricate and uneven Von Mises stress and strain patterns in the ligaments, along with mimicking the natural movement of the human knee joint when subjected to external loads. Few researchers have examined and summarized the biomechanical properties of the major ligaments of the knee joint under various motion conditions. To address this gap, our study utilized software tools like Mimics, Geomagic, and ANSYS to create and validate a 3D model based on MRI images of a healthy male's left knee joint. The goal of our study was to examine Von Mises stress data for ACL, PCL, MCL and LCL during anterior, posterior, and lateral impacts on different parts of the knee joint in a static standing position. By simulating impact loading on the upper, middle, and lower parts of the knee joint using FEA software, and analyzing the specific damage to four ligaments based on acquired stress–strain data, we can determine which ligament sustains the greatest damage under various impact directions and locations. This information can provide recommendations for protective measures for athletes' knee joints, potentially aiding in better protection and injury prevention. Furthermore, identifying the most vulnerable ligament from data on ligament damage under different impact scenarios may offer a theoretical basis for diagnosing and rehabilitating knee joint ligament injuries in clinical settings.

Materials and methods

Knee joint imaging materials

An adult Chinese volunteer (male, weighing 70 kg) with no history of prior knee injury or osteoarthritis was selected. The left knee joint was scanned using a magnetic resonance scanner (Achieva 1.5 T, PHILIPS, Netherlands). The scan had a slice thickness of 2 mm and a slice increment of 1 mm, resulting in a total of 152 images.

Geometry reconstruction

Mimics (medical finite element modeling software, 19.0, Materialise, Belgium), Geomagic Studio (reverse engineering software, 2012, Geomagic, USA), and ANSYS Workbench (finite element analysis processing software, 19.2, ANSYS, USA) were employed.

Using the functions of threshold segmentation, separation mask, edit mask, region growth, and 3D calculation in Mimics17, the original MRI data and the characteristics of different structural densities of the knee joint were utilized to generate a 3D model. This model encompasses various structures of the human knee joint, such as the femur, patella, tibia, fibula, femoral cartilage, tibial cartilage, patellar cartilage, fibular cartilage, meniscus, ACL, PCL, MCL, LCL, and PL. Each part of the model was saved in a standard surface subdivision format, and exported in Standard Triangle Language (STL) format (as shown in Fig. 2a).

The knee tissue structures were imported into Geomagic Studio 12.0 software. To improve the quality of the models, Smoothing Function was applied to eliminate nail-shaped objects, while the Mesh Doctor Function was used to fill small holes and channels and smooth highly refractive edges. Afterwards, to achieve a curved model, precise surface machining and automatic surface shaping techniques were employed for accurate results. In the automatic surface creation, the geometric image type was set to organic, and the target number of surfaces was set to 500. The final output was saved in Initial Graphics Exchange Specification (IGES) format.

Material and boundary conditions

We initiated the Statics Analysis module in Workbench, importing the.igs file, which was exported from Geomagic. The model underwent a Boolean operation to remove any overlap resulting from human error during the reconstruction process. Subsequently, we defined the material properties and contact types of the model, and executed mesh partitioning.

The assignment of elastic modulus and Poisson's ratio for the model is based on the research data from Li [17] and Bae [24]. This study simplifies the total knee joint model, designating the bone, meniscus, and articular cartilage of the model as isotropic linear elastic materials. To restore the nonlinearity and large deformation rate of ligaments, Some studies [15, 25] have defined ligaments as hyperelastic materials and

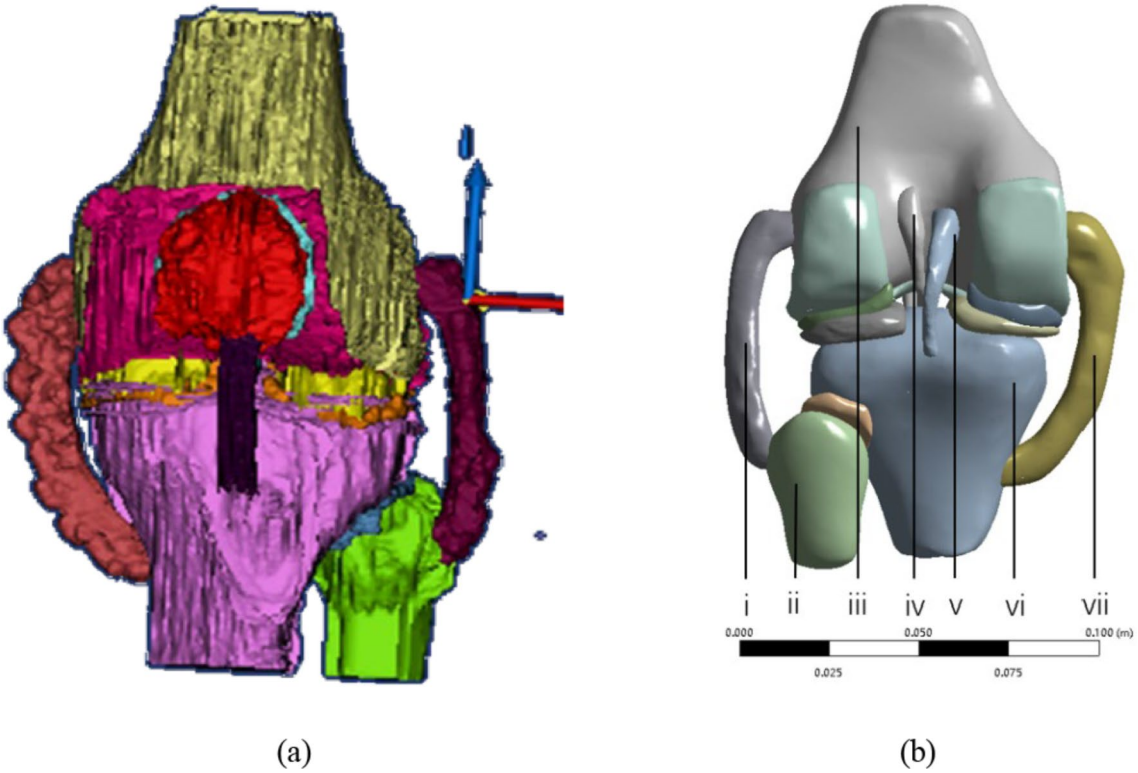

Fig. 2 Knee joint model **a** 3D reconstruction of knee joint; **b** The overall structure of the knee joint finite element model with (i) LCL, and (ii) Perone. (iii) Femur. (iv) ACL. (v) PCL. (vi) Tibia. (vii) MCL

used the Neo-Hooker model. However, in this study, linear elastic materials were chosen to simplify calculations and increase computational speed. Specific material parameter properties are detailed in Table 1.

The model was partitioned automatically using tetrahedral meshes, resulting in 93,465 nodes and 50,402 elements. Since the kinematic states of bone, articular cartilage, and ligaments were not the main focus of this study, their connections were all set to bonded when selecting the contact type. Meanwhile, the contact types between the articular cartilages, and between the meniscus and articular cartilage, are set to No Separation. The overall structure of the knee joint finite element model is depicted in Fig. 2b.

Table 1 material properties of knee joint tissues

Knee structure	Elastic Modulus /MPa	Poisson's ratio
Bone	12,000	0.3
Meniscus	59	0.49
Cartilage	5	0.46
ACL	116	0.3
PCL	87	0.3
MCL	48	0.3
LCL	48	0.3
PL	87	0.3

Model validation

The effectiveness of the knee joint model is verified using the following techniques:

Validation I: In previous studies, Chen [6], Hang [26], and Jin [8] conducted experiments where they applied vertical downward forces of 500N, 1000N, and 1150N on the knee joint in the extended position. These forces were used to simulate the human status in a stationary stance on a single leg or both legs. Bao [27], Moglo [28] validated the model with a 1,000 N load; Fukubayashi [29] tested cadaveric knee joint specimens in the extended position with vertical loads of 200, 500, 1,000, and 1,500 N to analyze load distribution on the cartilage and contact area. Using as reference from their research, a vertically downward force of 1000N is applied to the top surface of the femoral model. The bottom surfaces of the tibia and fibula are Fixed Support and constrained to six degrees of freedom, and the degrees of freedom of other structures controlled by ligaments. The specific position where the loads are applied is shown in Fig. 3a and b. This setup was used to calculate the equivalent stress of femoral cartilage, tibial cartilage, and meniscus.

Validation II: The anterior drawer test (ADT) is a common maneuver to assess ACL injuries. Following the standard set by Frobell [30] for the ADT, in Validation II, we used the tibial plateau bulge as a reference point. In certain clinical and existing literature [31, 32], a 134N forward load was utilized as a criterion for ADT. To facilitate intuitive comparison, we applied a 134 N force horizontally backward from the reference point. The specific position where the loads are applied is shown in Fig. 3c and d. Furthermore, the femoral top surface was fixed as the constraint condition. We then calculated the displacement of the tibia and the equivalent stress of ACL, PCL, MCL, and LCL.

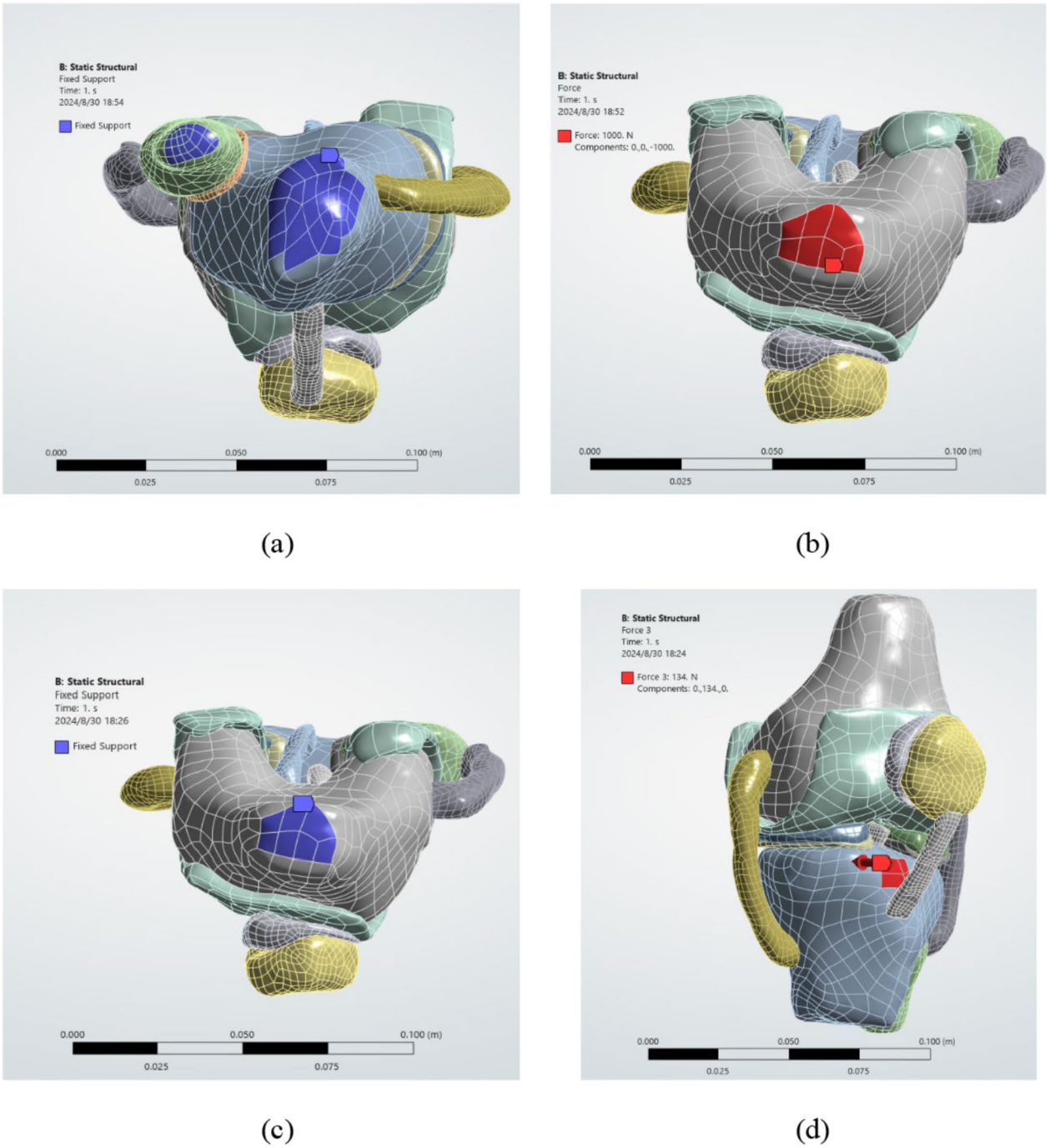

Fig. 3 Specific location of validated loads **a** Fixed support for Verification I; **b** Force load for Verification I; **c** Fixed support for Verification II; **d** Force load for Verification II

Impact simulation

Given the brief duration of impact in Taekwondo, this study assumed the athletes to be in a standing position at the moment of impact. According to the research data by Li [33], it was revealed that when human legs are stationary, the knee joint carries 43% of the body weight. Hence, it was estimated that the knee joint in this model beard a load of approximately 300N in a static standing position. This load was applied vertically downwards onto the top surface of the femoral model (Fig. 4a), while an additional load of 134N was applied towards the upper, middle, and lower sections of the knee joint from the front, back, and side (Fig. 5a–i). The upper, middle, and lower segments of the knee joint as defined in this study are primarily determined by the positions of the constituent bones. The specific definitions of the upper, middle, and lower portions of the knee are as follows: Upper knee joint: refers to the lower femur, the distal femur. Middle part of the knee: the core area where the lower femur, upper tibia, and patella interact. Lower knee part: the upper tibia, the proximal tibia.

When the upper and middle sections of the knee joint were impacted, the bottom surfaces of the tibia and fibula were fixed as constraints. Conversely, when the lower section of the knee joint was impacted, the top surface of the femur was fixed as constraints. The specific position where the Fix Supports are applied is shown in Fig. 4b–c. The equivalent stresses of ACL, PCL, MCL, and LCL during impact were then calculated.

Results

Results of model validation

Validation I results: Under a vertical load of 1000 N, the femoral cartilage experienced a maximum stress of 10.236 MPa, with the overall stress being higher medially than laterally. The maximum stress in the medial meniscus was 54.352 MPa, located at the anterior corner of the meniscus, while the maximum stress in the lateral meniscus was 35.267 MPa, situated at the posterior corner of the meniscus. The medial tibial cartilage had a maximum stress of 4.6336 MPa, located centrally, and the lateral tibial cartilage had a maximum stress of 4.1971 MPa, located at the anterior edge (refer to Fig. 6). The Von Mises stress distributions observed in the femoral cartilage, meniscus, and tibial cartilage when subjected to a vertical load of 1000 N applied to the total knee joint generally aligned with the finite element calculations conducted by Zhu [34].

Validation II results: Under an anterior load of 134 N, the maximum backward displacement of the tibia was 4.9129 mm. The maximum stresses in ACL, PCL, MCL, and LCL were 19.253 MPa, 5.0691 MPa, 1.7712 MPa, and 1.591 MPa respectively (refer to Fig. 7). The results obtained from a 134N anterior load validation also aligned with the findings of Li [17] and colleagues. By validating the model under two different conditions, its credibility has been established, allowing for further analysis of the ligaments' equivalent force data in various impact scenarios.

Stress analysis

Figures 8, 9, 10 and 11 illustrates the stress distribution patterns of the ACL, PCL, MCL, and LCL in nine impact scenarios on the human knee joint while in a static standing position with both legs. Furthermore, to visualize the relationship between the stress exhibited on the ligaments and the risk of ligament injury, we calculated the maximum stress data of each ligament under different

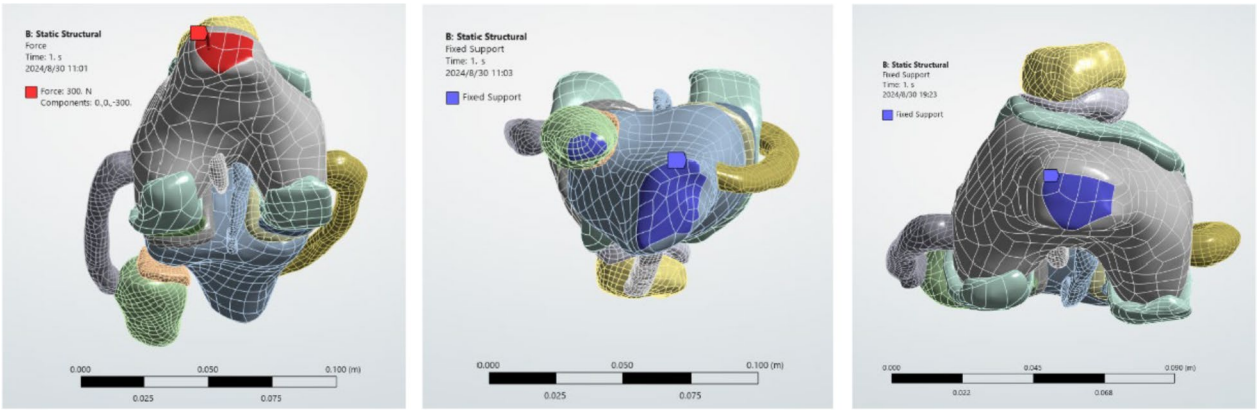

Fig. 4 Base loads applied to the model in a static standing position **a** A vertically downward force load of 300N; **b** Fixed supports in case of impacts on the upper and middle parts; **c** Fixed supports in case of impacts on the lower parts

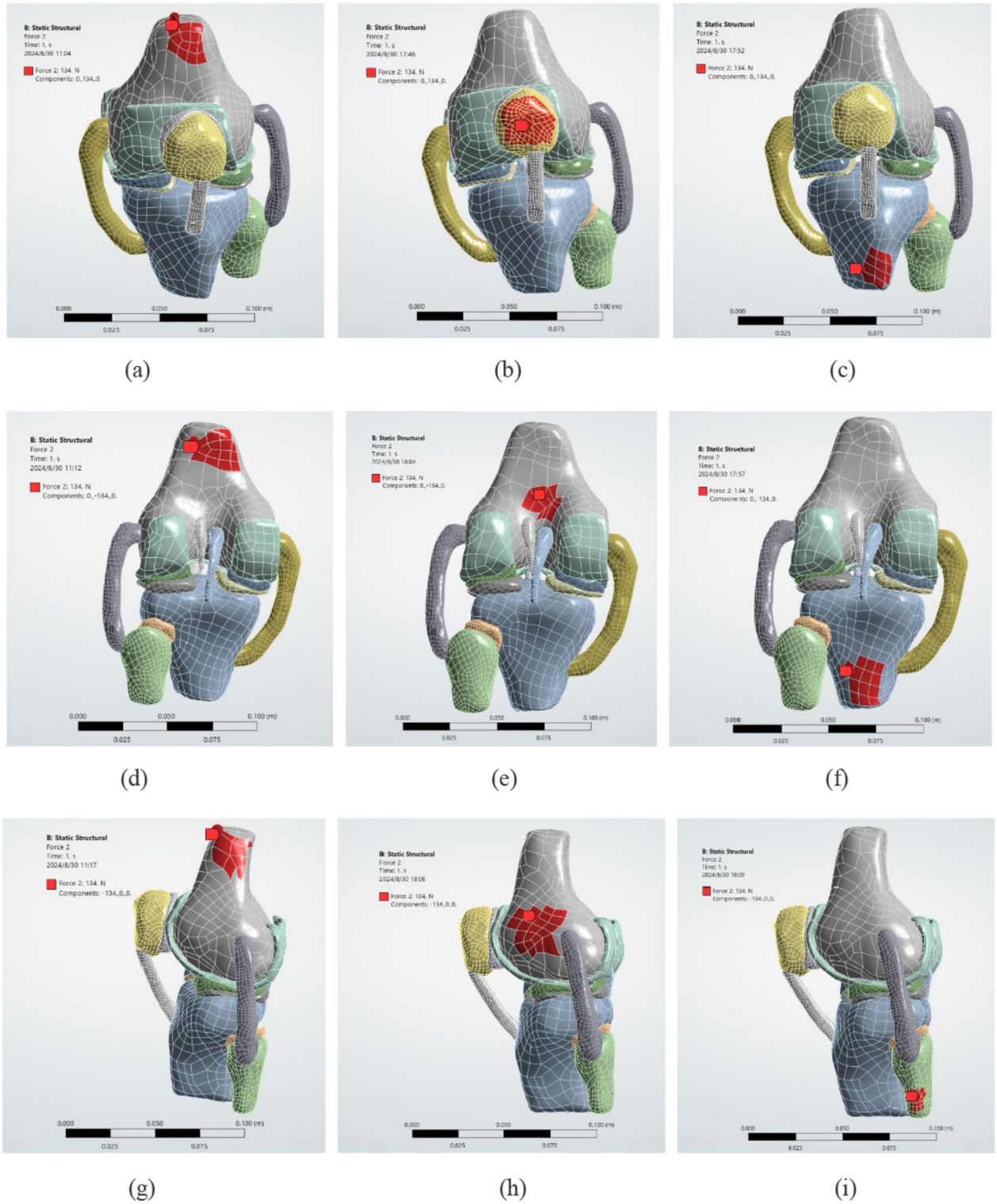

Fig. 5 The position where the load impacts the knee joint **a** upper subjected to anterior impact; **b** middle subjected to anterior impact; **c** lower subjected to anterior impact; **d** upper subjected to posterior impact; **e** middle subjected to posterior impact; **f** lower subjected to posterior impact; **g** upper subjected to lateral impact; **h** middle subjected to lateral impact; **i** lower subjected to lateral impact

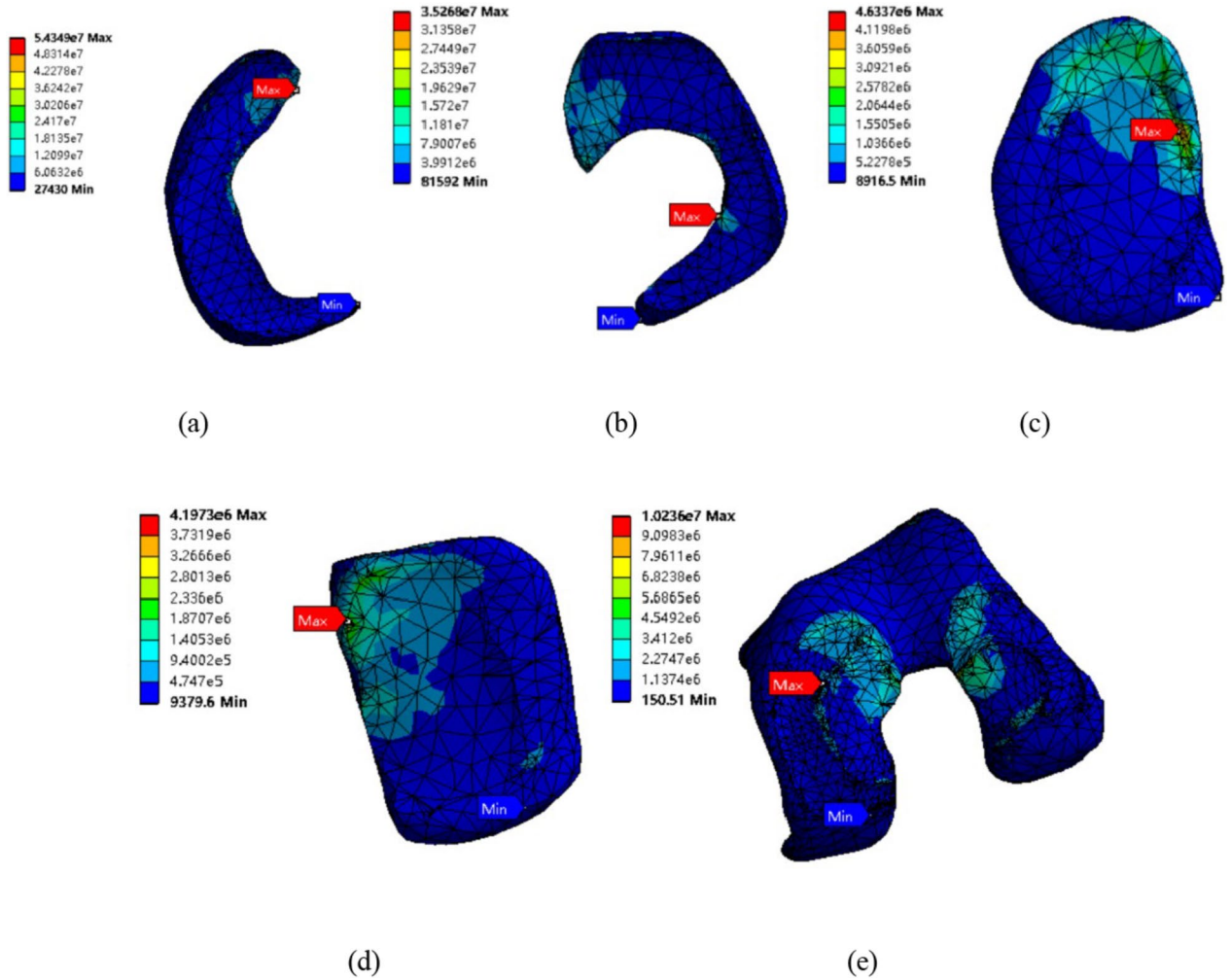

Fig. 6 The Von Mises stress distributions of the result of validation I; **a** The Von Mises stress distribution of medial meniscus; **b** The Von Mises stress distribution of lateral meniscus; **c** The Von Mises stress distribution of Medial tibial cartilage; **d** The Von Mises stress distribution of Lateral tibial cartilage; **e** The Von Mises stress distribution of Femoral cartilage

impact conditions based on the ultimate stress results of ACL, PCL, LCL, and MCL obtained from Ristaniemi's study [35], as well as the ratio of the maximum stress to the ultimate stress of each ligament. The approximate percentage values are listed in Table 2.

By comparing the Von Mises stress distribution of the ligaments under different impact conditions, we obtained: When the knee joint was impacted from the front and back, the PCL experienced the highest amount of stress, particularly at the junction between the PCL and the tibia. During anterior impacts, the PCL experienced maximum stresses of 59.895 MPa, 27.481 MPa, and 28.607 MPa, while during posterior impacts, the maximum stresses on the PCL were 57.421 MPa, 38.147 MPa, and 26.904 MPa in that order. Similarly, in the case of a side impact on the upper and middle knee, the ACL bore the maximum force at 32.102 MPa and 29.544 MPa respectively, with the peak force occurring at the ACL-tibia junction. Furthermore, in the case of lateral impact on the lower part of the knee joint, the LCL sustained the maximum force at 22.279 MPa, with the peak force situated at the LCL-fibula junction.

In terms of specific forces experienced on each ligament, the ACL was subjected to the highest force of 36.415 MPa when the upper part of the knee was impacted from the back. Conversely, the PCL experienced the highest force of 59.895 MPa when the upper part of the knee was impacted from the front. When a side impact affected the upper part of the knee, the MCL received the highest force of 28.86 MPa, whereas the LCL was most stressed during lateral impact on the lower part of the knee joint, with 22.279 MPa.

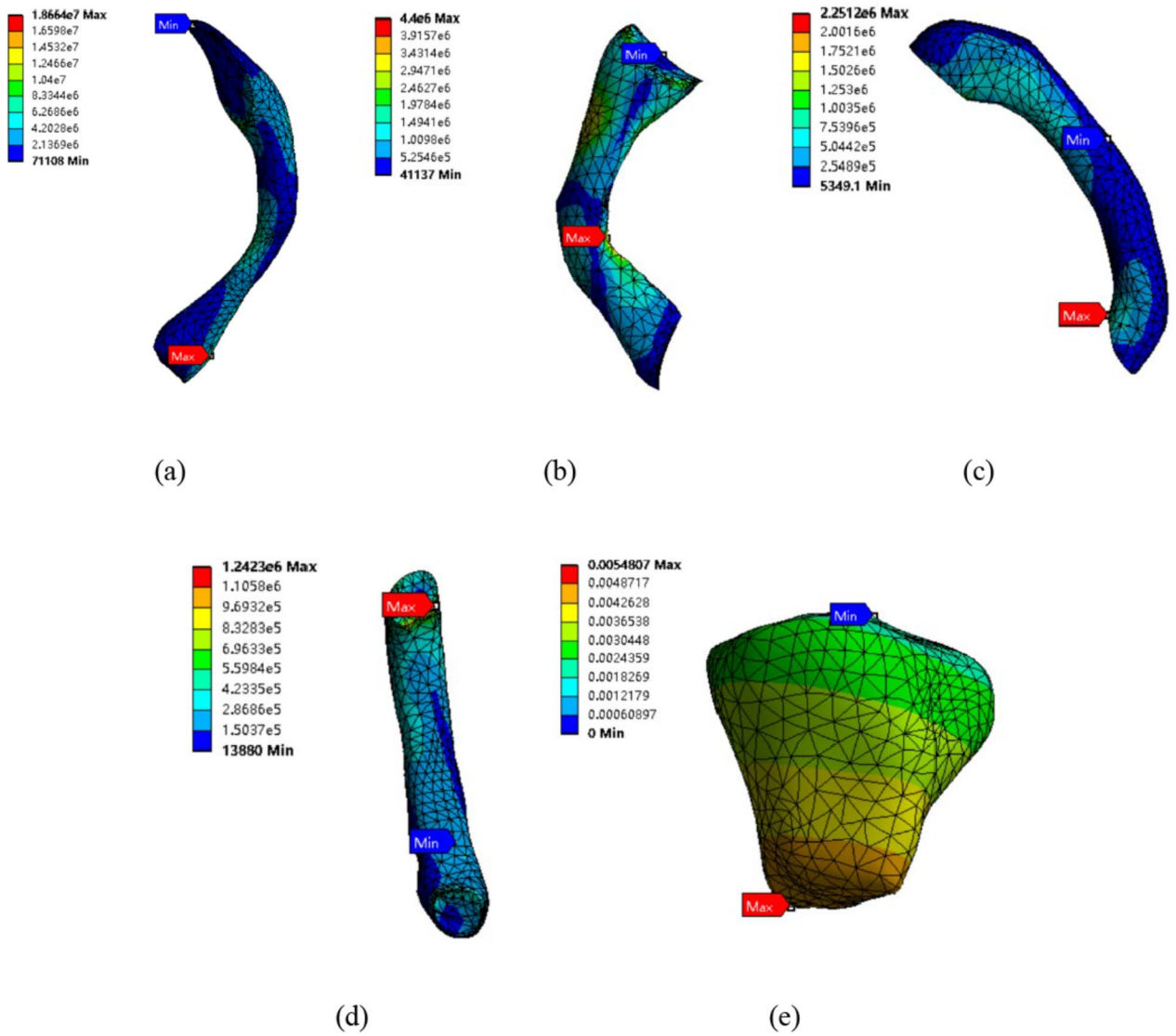

Fig. 7 The Von Mises stress distributions of the result of validation II; **a** The Von Mises stress distribution of ACL; **b** The Von Mises stress distribution of PCL; **c** The Von Mises stress distribution of MCL; **d** The Von Mises stress distribution of LCL; **e** The total deformation of tibia

It is evident that under the same impact condition, ACL and PCL are more susceptible to injury compared to the other two ligaments. When the upper part of the knee joint is impacted from the rear, the maximum stress exhibited by the ACL reaches 138% of its ultimate stress. On the other hand, when the upper part of the knee joint is impacted from the front, the maximum stress on the PCL reaches 200% of its ultimate stress, posing a significant risk of rupture. In contrast, the stresses exhibited by MCL and LCL under all conditions do not exceed their respective ultimate stresses.

Next, we proceed with the injury analysis of ligaments under various impact conditions based on Table 2. Our initial step involves eliminating the groups where the stress experienced by the ligaments exceeds their ultimate stresses. Upon comparing the remaining groups, we found that the group subjected to lateral impact at the lower part exhibited the lowest risk of damage (ratio ACL 38%, PCL 23%, MCL 10% and LCL 62%). Overall, the knee joint appears to be less vulnerable to injury when subjected to external forces impacting its lower part, compared to impacts on its middle or upper parts.

Several research results [36–39] have shown that the ACL, PCL, and MCL may all be injured due to direct impact on the knee joint. LCL injuries are the least common among knee ligament injuries, accounting for approximately 4% of all cases [40]. The lower incidence of LCL injuries compared to other knee ligaments aligns with the findings of this study.

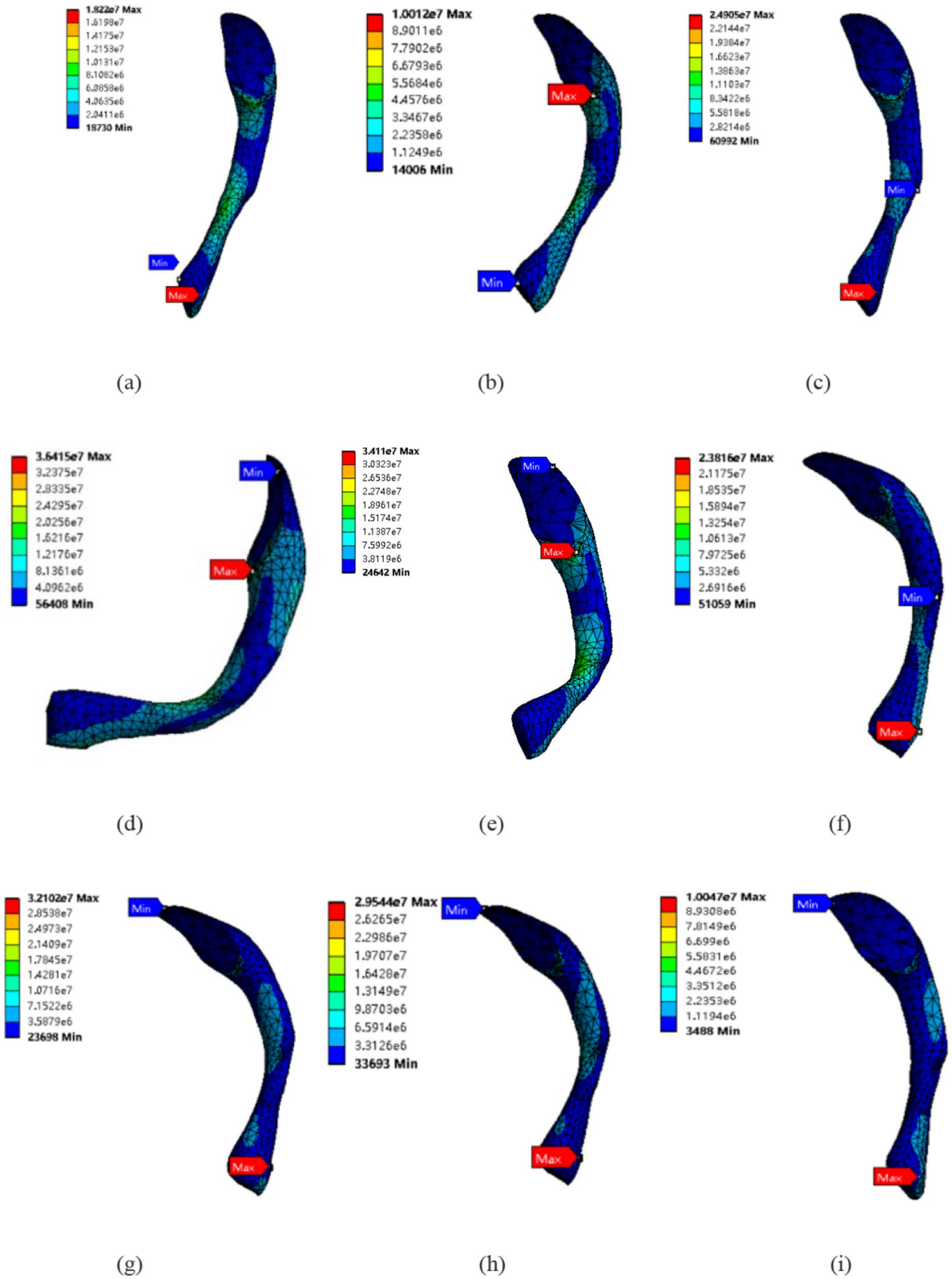

Fig. 8 The Von Mises stress distribution of the ACL when the knee is impacted by all sides; **a** upper subjected to anterior impact; **b** middle subjected to anterior impact; **c** lower subjected to anterior impact; **d** upper subjected to posterior impact; **e** middle subjected to posterior impact; **f** lower subjected to posterior impact; **g** upper subjected to lateral impact; **h** middle subjected to lateral impact; **i** lower subjected to lateral impact

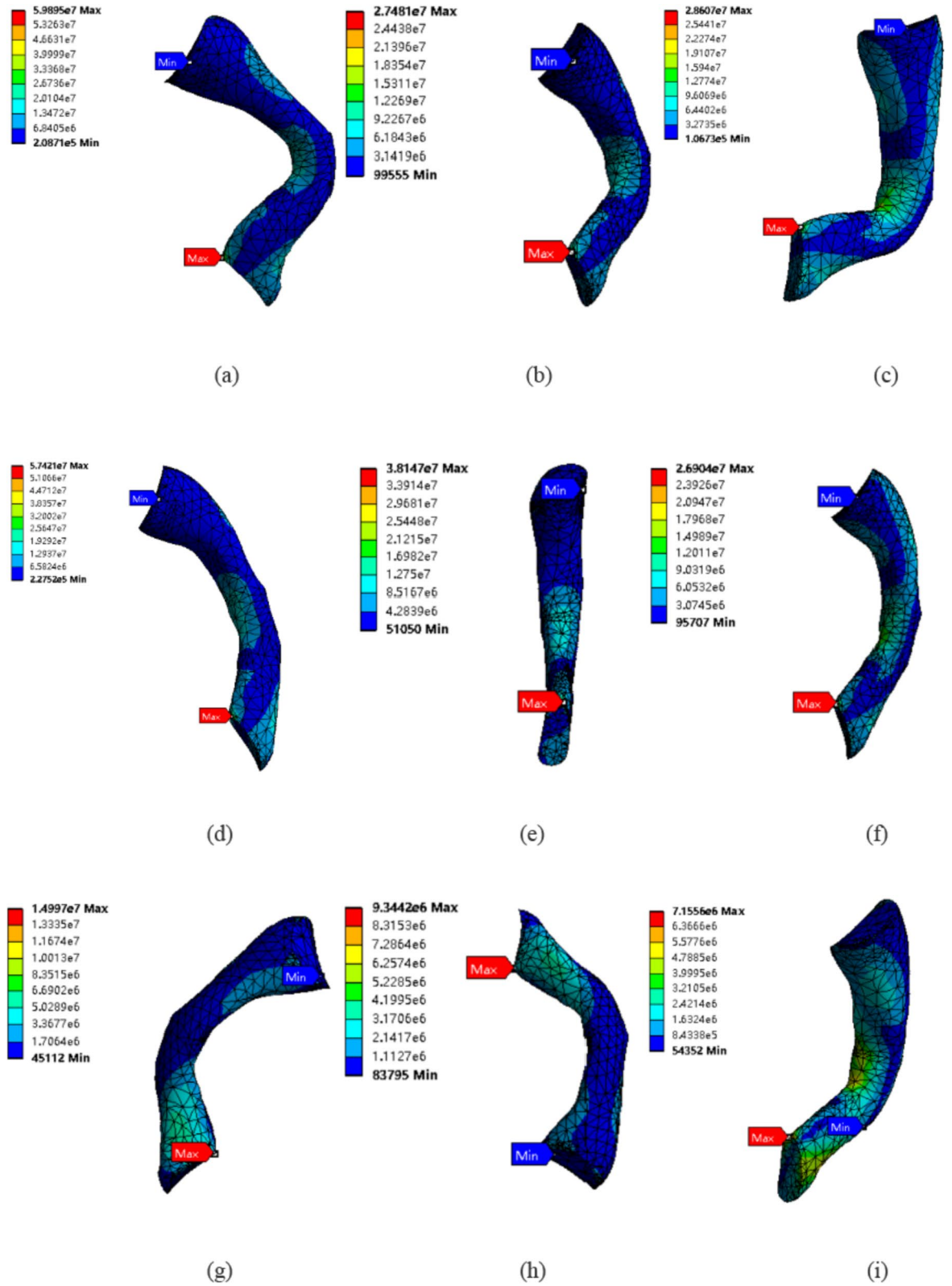

Fig. 9 The Von Mises stress distribution of the PCL when the knee is impacted by all sides; **a** upper subjected to anterior impact; **b** middle subjected to anterior impact; **c** lower subjected to anterior impact; **d** upper subjected to posterior impact; **e** middle subjected to posterior impact; **f** lower subjected to posterior impact; **g** upper subjected to lateral impact; **h** middle subjected to lateral impact; **i** lower subjected to lateral impact

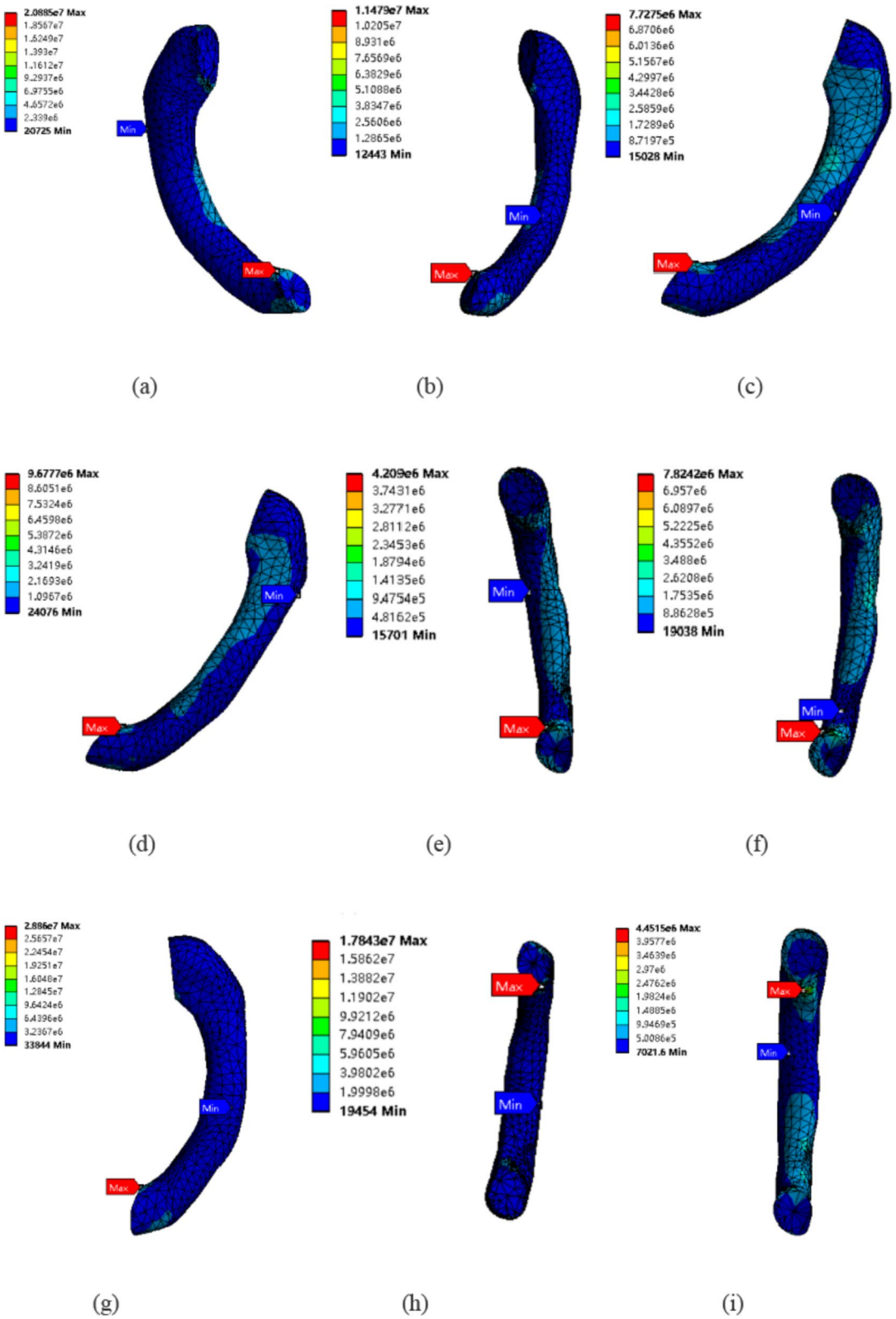

Fig. 10 The Von Mises stress distribution of the MCL when the knee is impacted by all sides; **a** upper subjected to anterior impact; **b** middle subjected to anterior impact; **c** lower subjected to anterior impact; **d** upper subjected to posterior impact; **e** middle subjected to posterior impact; **f** lower subjected to posterior impact; **g** upper subjected to lateral impact; **h** middle subjected to lateral impact; **i** lower subjected to lateral impact

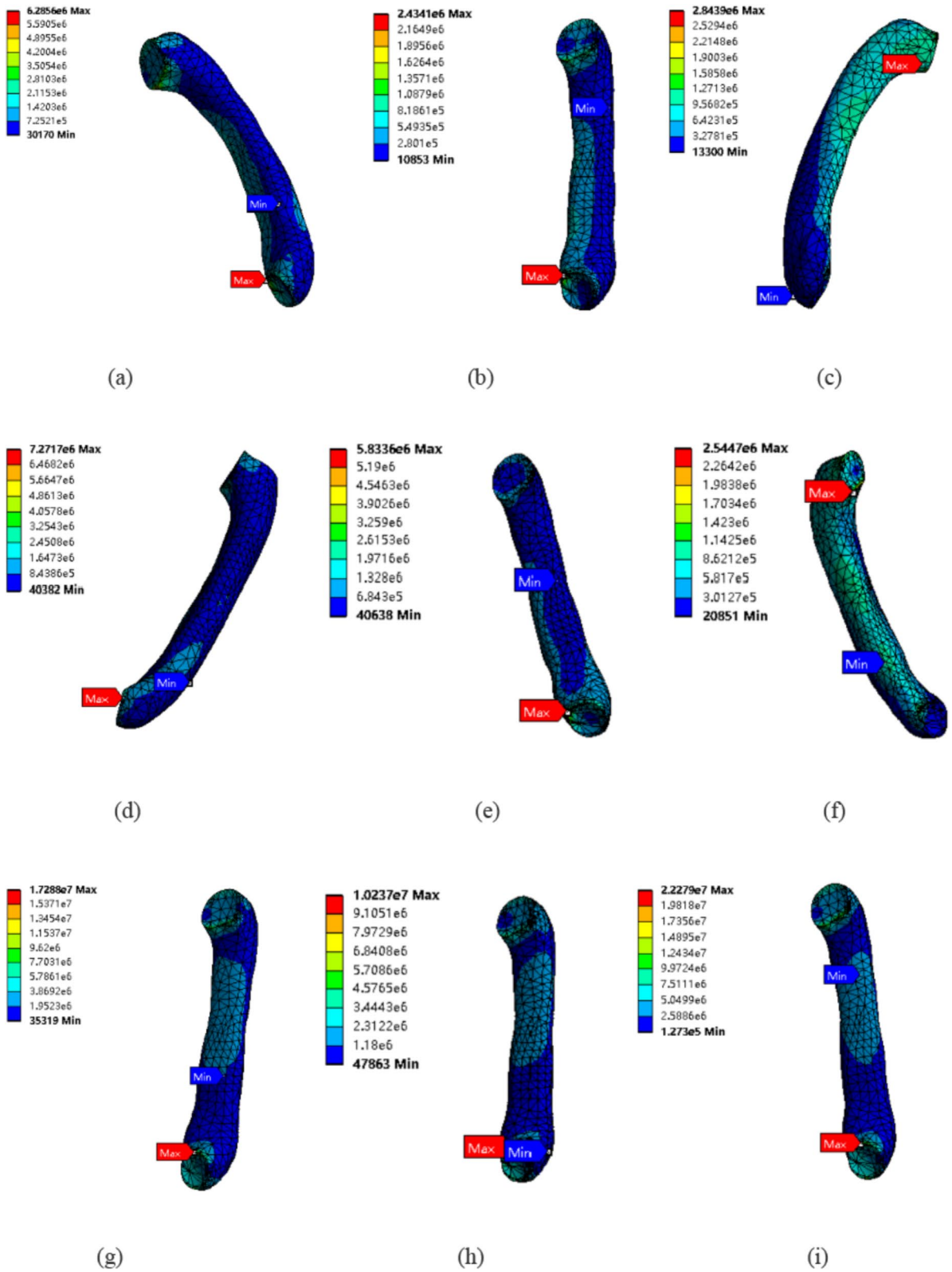

Fig. 11 The Von Mises stress distribution of the LCL when the knee is impacted by all sides; **a** upper subjected to anterior impact; **b** middle subjected to anterior impact; **c** lower subjected to anterior impact; **d** upper subjected to posterior impact; **e** middle subjected to posterior impact; **f** lower subjected to posterior impact; **g** upper subjected to lateral impact; **h** middle subjected to lateral impact; **i** lower subjected to lateral impact

Table 2 Maximum stress of knee ligaments under different impact conditions

Impact situation	The Von Mises stress of each ligament when the knee joint is impacted (MPa) (The ratio of this stress in relation to the ultimate stress) [35]			
	ACL	PCL	MCL	LCL
Upper section impacted from the front	18.22(70%)	59.895(200%)	20.885(49%)	6.2856(18%)
Middle section impacted from the front	10.012(38%)	27.481(90%)	11.479(25%)	2.4341(5%)
Lower section impacted from the front	24.905(92%)	28.607(93%)	7.7275(16%)	2.8439(8%)
Upper section impacted from the rear	36.415(138%)	57.421(190%)	9.6777(23%)	7.2717(20%)
Middle section impacted from the rear	34.11(130%)	38.147(126%)	4.209(9%)	5.8336(17%)
Lower section impacted from the rear	23.816(88%)	26.904(86%)	7.8242(18%)	2.5447(5%)
Upper section impacted from the side	32.102(123%)	14.997(46%)	28.86(65%)	17.288(48%)
Middle section impacted from the side	29.544(111%)	9.3442(31%)	17.843(41%)	10.237(28%)
Lower section impacted from the side	10.047(38%)	7.1556(23%)	4.4515(10%)	22.279(62%)

Discussion

FEA approximates an infinite number of unknowns with a finite number of unknowns, simplifying a complex problem for solution. In knee studies, FEA can simulate the mechanical behavior of the knee joint during various motion states [41–44], and also represent the stress -strain impact on the knee joint in conditions like fracture [45–48], knee arthroplasty [49–51], and osteoarthritis [52–54]. In comparison to experimental studies, FEA is more time- and cost-effective. It can predict Von Mises stress and strain distributions under various conditions based on experimental results, aiding in the design and optimization of medical devices like knee prostheses. Although the FEA method has its advantages, it also comes with drawbacks. The analysis outcomes can be influenced by factors such as model geometry, boundary conditions, material properties, and other parameters. The precision of the model significantly influences the reliability of the results. Above all, performing calculations to simulate complex biomechanical systems is time-consuming, demanding high computer performance.

Therefore, FEA can be a valuable tool in knee-related research, but it must be utilized considering its advantages and limitations. In the field of knee joint biomechanics research, numerous scholars are dedicated to enhancing the 3D model of the knee joint. Zhang [55] employed medical image processing technology to reconstruct the solid model of bone tissue and soft tissue of the knee joint separately. They utilized 3D image alignment technology to integrate each soft tissue group onto the solid model of bone tissue, creating a comprehensive knee joint incorporating all bone tissues and major soft tissues. This process resulted in the formation of a geometric surface anatomical digital model, enhancing the accuracy of geometric shape simulation. Zhao [56] combined computerized motion simulation technology with a simulation model of postoperative motion mechanics after knee arthroplasty to lay the groundwork for optimizing knee prosthesis data. The dynamic features of the healthy knee joint are valuable for designing knee prostheses and treating osteoarthritis. Dynamic modeling involves analyzing mechanical properties and kinematic parameters during motion. However, the intricate anatomy of the knee joint and the interaction with body dynamics pose challenges in understanding its detailed dynamic properties. For this, scientists [57] have developed a specialized musculoskeletal model and a precise finite element model of the complete knee joint to analyze its kinematics and mechanics throughout the gait cycle. This also serves as a valuable tool for evaluating mechanical properties at both body and tissue levels.

In biomechanical studies of knee ligaments, most scholars choose to analyze a single ligament, for instance, Huang [58] and He [59] conducted research on ACL and MCL, and systematic comparative analyses of the entire knee joint or all ligaments are uncommon. In this study, a biomechanical FEA of the four main knee joint ligaments was conducted to investigate the effects of various types of impacts. By integrating findings from previous studies, this approach helps to mitigate the constraints of individual ligament investigations to some degree. Mimics and Geomagic software were utilized for processing MRI images, extracting bone, cartilage, and certain ligaments, and performing 3D stereo model reconstruction of the human knee joint. Two validation methods were subsequently used in Ansys to verify the model's validity. Based on the validation results, we compared and analyzed nine cases where the upper, middle, and lower parts of the knee joint experienced anterior, posterior, and lateral impacts in the static standing state of the human leg. Von Mises stress cloud diagrams were created for the cruciate ligament and the medial collateral ligament.

Next, some discussion will be presented on the design of the study, the results, and the direction of future optimization research. We have divided the knee joint into upper, middle, and lower parts, but it is important to note that these divisions are not strict anatomical concepts as the knee joint itself is a holistic structure without clear boundaries. Based on this, our definition of these parts is primarily based on the relative positions of the constituent bones. In the field of biomechanics, different anatomical structures exhibit distinct biomechanical properties under the same loading conditions. To interrogate the disparities in biomechanical characteristics of knee ligaments stemming from variations in impact direction and the localized site of impact, we integrated scenarios of potential sudden impacts encountered in daily life with this stratified approach to impacted areas. It is imperative to underscore, in the context of knee joint research, that the knee joint, as an integrated structure, intricately interconnects and interacts with its various components, collectively sustaining the joint's normal functionality and stability. Consequently, when contemplating and elucidating the knee joint, a holistic perspective that encompasses its comprehensive biomechanical properties is paramount.

Additionally, we chose max stresses as the main data for inter-group comparison in our experimental design because the locus of peak stress, frequently identified as the region or site experiencing the greatest loading intensity within a stressed structure or object, often predicts the onset of deformation, rupture, or functional failure. As Ren's research [15] elucidates, this peak stress location precisely aligns with the clinically prevalent site of anterior cruciate ligament (ACL) rupture. Consequently, the stress maximum emerges as a precise quantitative metric, facilitating more intuitive intergroup comparisons that comprehensively illustrate and analyze stress distributions across distinct locations and loading orientations, thereby enhancing our understanding of stress-related phenomena in biomechanical systems.

An examination of the stress data presented herein underscores that when the upper portion of the knee joint is subjected to impact, the maximum stresses exhibited by the ligaments surpass those observed in the lower and middle segments of the joint. This observation underscores the imperative to mitigate impacts to the upper knee region, as they may precipitate excessive stress concentrations with potentially deleterious consequences for ligament integrity. In addition, the knee joint model was simplified and lacked tissues such as muscles and tendons, and the material property division could be more refined.

Finally, we will discuss the limitations and potential improvements of this study. Our knee joint model was simplified and lacked tissues such as muscles and tendons, and the material property division could be more refined. There is a study [60] that has revealed that variations in ligament mechanics in knee joint models stem primarily from distinctions in geometry, boundary conditions, and ligament modeling parameters rather than from soft-tissue structures like muscles. In this study, we examine the applied impact as an instant static load to analyze the biomechanical alterations and reaction of the knee joint at that moment. While the muscles surrounding the knee joint typically respond to maintain joint stability and equilibrium when facing an impact, the author suggests that in the context of the instantaneous static impact studied, the muscles may not exhibit changes like contraction to counter the external force, but rather aim to diminish resistance and absorb a portion of the impact force. Due to these considerations, and to optimize computational resources and speed up computations, this study's model simplifies the muscle component. Future research will reconstruct a detailed musculoskeletal model of the knee joint to conduct transient finite element analyses, enabling a comparison and discussion of the muscles' role in ligament mechanics when the knee joint is impacted.

Our study examines the static mechanics of the knee joint in the static standing state of both legs. In the future, it could be utilized to investigate ligament damage in the knee joint during flexion and walking under external impact, and to simulate potential ligament damage during sports activities. It is anticipated that as science and technology advance and researchers continue their efforts, human research on the knee joint will become more thorough and precise, leading to a reduction in knee injuries.

Conclusions

The findings of this research align with the physiological traits and clinical observations of the human knee. These outcomes could establish a theoretical groundwork for averting ligament trauma in the knee due to sudden impacts and for managing such injuries clinically. Recommendations include prioritizing the protection of the upper knee area from impacts in various directions during external blows or confrontations and leveraging the middle and lower sections of the knee to absorb the force. This approach may lower ligament injury risks and provide some degree of knee joint protection. We also recommend that scholars exploring this topic, consider incorporating injuries like knee external and internal rotation into their research to enhance the clinical relevance of knee injury studies.

Acknowledgements
Not applicable.

Author contributions
LJ: Conceptualization, Software, Methodology, Supervision, Writing—Review & Editing. LHB: Writing—Original Draft, Review and Editing, Conceptualization and Validation. SMY: Data Curation, Investigation and Conceptualization. LF: Writing—Software Provided, Resources. ZZY: Writing—Visualization, ensuring that the descriptions are accurate and agreed. WZH: Writing—Software Provided, Resources. HLM: Conceptualization, Writing—Review & Editing. ZGA: Writing—Resources. RW: Writing—Review & Editing, Project Administration, Funding Acquisition.

Funding
This work was supported by Key Scientific Research Project of Universities in Henan Province (22A416001), Henan Province Foundation for University Key Teacher (2021GGJS102), The open project program of the first hospital of Xinxiang Medical University (XZZX2022005), Scientific Research Innovation Project of Xinxiang Medical University Students (xskjzzd202356), Henan Provincial Medical Science and Technology Tackling Plan Joint Construction Project (LHGJ20220609).

Availability of data and materials
No datasets were generated or analysed during the current study.

Declarations

Competing interests
The authors declare no competing interests.

Consent for publication
Not applicable.

Author details
[1]The First Afiliated Hospital of Xinxiang Medical University, School of Medical Engineering, Xinxiang Medical University, Xinxiang 453003, China. [2]Engineering Technology Research Center of Neurosense and Control of Henan Province, Henan Engineering Research Center of Medical VR Intelligent Sensing Feedback, Xinxiang Engineering Technology Research Center of Intelligent Rehabilitation Equipment, Xinxiang 453003, China.

Received: 29 April 2024 Accepted: 7 September 2024
Published online: 07 October 2024

References

1. Flandry F, Hommel G. Normal anatomy and biomechanics of the knee. Sports Med Arthrosc Rev. 2011;19(2):82–92. https://doi.org/10.1097/JSA.0b013e318210c0aa.
2. Ji M. Analysis of injuries in taekwondo athletes. J Phys Ther Sci. 2016;28(1):231–4. https://doi.org/10.1589/jpts.28.231.
3. Wang T. Research on knee joint injury of Taekwondo Athletes. LaoQuJianShe. 2011;20:43–6 (**In Chinese**).
4. Moeinzadeh MH, Engin AE, Akkas N. Two-dimensional dynamic modelling of human knee joint. J Biomech. 1983;16(4):253–64. https://doi.org/10.1016/0021-9290(83)90133-1.
5. Li G, Gil J, Kanamori A, et al. A validated three-dimensional computational model of a human knee joint. J Biomech Eng. 1999;121(6):657–62. https://doi.org/10.1115/1.2800871.
6. Chen Y, Lu C, Zhao Y, et al. Construction and simulation mechanical analysis of dynamic knee joint finite element model based on CT image. Zhongguo Gu Shang. 2020;33(5):479–84. https://doi.org/10.12200/j.issn.1003-0034.2020.05.018.
7. Madeti BK, Chalamalasetti SR, Bolla Pragada SS. Biomechanics of knee joint—a review. Front Mech Eng. 2015;10:176–86. https://doi.org/10.1007/s11465-014-0306-x.
8. Jin B, Hu Y, Han L. Establishment of 3D finite element model of meniscus and its mechanical analysis. China J Orthop Traumatol. 2020;33(8):766–70 (**In Chinese**).
9. Ding K, Yang W, Wang H, et al. Finite element analysis of biomechanical effects of residual varus/valgus malunion after femoral fracture on knee joint. Int Orthop. 2021;45(7):1827–35. https://doi.org/10.1007/s00264-021-05039-9.
10. Donahue TL, Hull ML, Rashid MM, et al. A finite element model of the human knee joint for the study of tibio-femoral contact. J Biomech Eng. 2002;124(3):273–80. https://doi.org/10.1115/1.1470171.
11. Shao B, Xing J, Zhao B, et al. Role of the proximal tibiofibular joint on the biomechanics of the knee joint: a three-dimensional finite element analysis. Injury. 2022;53(7):2446–53. https://doi.org/10.1016/j.injury.2022.05.027.
12. Mercan N, Yıldırım A, Dere Y. Biomechanical analysis of tibiofibular syndesmosis injury fixation methods: a finite element analysis. J Foot Ankle Surg. 2023;62(1):107–14. https://doi.org/10.1053/j.jfas.2022.05.007.
13. Li G, Suggs J, Gill T. The effect of anterior cruciate ligament injury on knee joint function under a simulated muscle load: a three-dimensional computational simulation. Ann Biomed Eng. 2002;30(5):713–20. https://doi.org/10.1114/1.1484219.
14. Benos L, Stanev D, Spyrou L, Moustakas K, Tsaopoulos DE. A review on finite element modeling and simulation of the anterior cruciate ligament reconstruction. Front Bioeng Biotechnol. 2020;20(8):967. https://doi.org/10.3389/fbioe.2020.00967.
15. Ren S, Shi H, Liu Z, et al. Finite element analysis and experimental validation of the anterior cruciate ligament and implications for the injury mechanism. Bioengineering. 2022;9(10):590. https://doi.org/10.3390/bioengineering9100590.
16. Sanchis-Alfonso V, Alastruey-López D, Ginovart G, et al. Parametric finite element model of medial patellofemoral ligament reconstruction model development and clinical validation. J Exp Orthop. 2019;6(1):32. https://doi.org/10.1186/s40634-019-0200-x.
17. Li Z, Liu L, Gao L, et al. Establishment and validation of precise finite element model of human total knee joint. Biomed Eng Clin Med. 2020;24(5):501–7. https://doi.org/10.13339/j.cnki.sglc.20200819.013. (**In Chinese**).
18. Peña E, Calvo B, Martínez MA, et al. A three-dimensional finite element analysis of the combined behavior of ligaments and menisci in the healthy human knee joint. J Biomech. 2006;39(9):1686–701. https://doi.org/10.1016/j.jbiomech.2005.04.030.
19. Yang S, Liu Y, Ma S, et al. Stress and strain changes of the anterior cruciate ligament at different knee flexion angles: a three-dimensional finite element study. J Orthop Sci. 2023. https://doi.org/10.1016/j.jos.2023.05.015.
20. Jiang Y, Lu T, Xu B, et al. Stress changes of knee joint with different degrees of medial collateral ligament injury. Chinese J Tissue Eng Res. 2024;28(33):5270–5 (**In Chinese**).
21. Safari M, Shojaei S, Tehrani P, et al. A patient-specific finite element analysis of the anterior cruciate ligament under different flexion angles. J Back Musculoskelet Rehabil. 2020;33(5):811–5. https://doi.org/10.3233/BMR-191505.
22. Seo YJ, Song SY, Kim IS, et al. Graft tension of the posterior cruciate ligament using a finite element model. Knee Surg Sports Traumatol Arthrosc. 2014;22(9):2057–63. https://doi.org/10.1007/s00167-013-2609-6.
23. Wang H, Tao M, Shi Q, et al. Graft diameter should reflect the size of the native anterior cruciate ligament (ACL) to improve the outcome of ACL reconstruction: a finite element analysis. Bioengineering. 2022;9(10):507. https://doi.org/10.3390/bioengineering9100507.
24. Bae JY, Park KS, Seon JK, et al. Biomechanical analysis of the effects of medial meniscectomy on degenerative osteoarthritis. Med Biol Eng Comput. 2012;50(1):53–60. https://doi.org/10.1007/s11517-011-0840-1.
25. He C, He W, Li Y, et al. Biomechanics of knee joints after anterior cruciate ligament reconstruction. J Knee Surg. 2018;31(4):352–8. https://doi.org/10.1055/s-0037-1603799.
26. Hang S, Zhang W, Wang T, et al. Establishment of finite element model of knee joint based on CT and MRI and analysis of biomechanical characteristics under different loads. Chin J Med Phys. 2021;38(3):370–4 (**In Chinese**).
27. Bao HRC, Zhu D, Gong H, et al. The effect of complete radial lateral meniscus posterior root tear on the knee contact mechanics: a finite element analysis. J Orthop Sci. 2013;18(2):256–63. https://doi.org/10.1007/s00776-012-0334-5.
28. Moglo KE, Shirazi-Adl A. Biomechanics of passive knee joint in drawer: load transmission in intact and ACL -deficient joints. Knee. 2003;10(3):265–76. https://doi.org/10.1016/s0968-0160(02)00135-7.

29. Fukubayashi T, Kurosawa H. The contact area and pressure distribution pattern of the knee: a study of normal and osteoarthrotic knee joints. Acta Orthop Scand. 1980;51(1–6):871–9. https://doi.org/10.3109/17453678008990887.
30. Frobell RB, Roos HP, Roos EM, et al. Treatment for acute anterior cruciate ligament tear: 5 year outcome of randomised trial. Br J Sports Med. 2015;49(10):700. https://doi.org/10.1136/bjsports-2014-f232rep.
31. Suggs J, Wang C, Li G. The effect of graft stiffness on knee joint biomechanics after ACL reconstruction-a 3D computational simulation. Clin Biomech. 2003;18(1):35–43. https://doi.org/10.1016/s0268-0033(02)00137-7.
32. He L, Li Y, Yu H, et al. Three-dimensional reconstruction algorithm-based magnetic resonance imaging evaluation of biomechanical changes in articular cartilage in patients after anterior cruciate ligament reconstruction. Comput Intell Neurosci. 2022;2022:8256450. https://doi.org/10.1155/2022/8256450.
33. Li G. Mechanical property analysis based on the modeling human knee articular. Heilongjiang: Harbin Institute of Technology, 2010. https://kns.cnki.net/kcms2/article/abstract?v=yqeyU9EK6jTlz3e65EgOK5aZDRKwEzgWuEUOHkY3E1yFMEX5WdGN8fF2hslKyesGlY3DtBzl3fm9EZwWeDse9VLE8eSBWooZg80Glsc0PrlygCUboOtlKr1gZh987uDGPDH4YRqFBQRNrsxlW3vKaA==uniplatform=NZKPTlanguage=CHS. (In Chinese).
34. Zhu G. Finite element analysis of Joint replacement of the single condyle knee. Beijing: Peking Union Medical College, 2016. https://kns.cnki.net/kcms2/article/abstract?v=yqeyU9EK6jRzei3glfmU7lC5dpCTKgN3CPVz89MddwMAWrLwIAlOezflGiaDmPommEkdaWx7q38iOUnuIxw3XJ2vY5auqPVNBAE-2nOMbyJVzbD0po2dZ0n2_q7ZuWKWse-5kRy-QXcSNNwAY4PJGw==uniplatform=NZKPTlanguage=CHS. (In Chinese).
35. Ristaniemi A, Stenroth L, Mikkonen S, Korhonen RK. Comparison of elastic, viscoelastic and failure tensile material properties of knee ligaments and patellar tendon. J Biomech. 2018;79:31–8. https://doi.org/10.1016/j.jbiomech.2018.07.031.
36. Shimokochi Y, Shultz SJ. Mechanisms of noncontact anterior cruciate ligament injury. J Athl Train. 2008;43:396–408. https://doi.org/10.4085/1062-6050-43.4.396.
37. Schulz MS, Russe K, Weiler A, Eichhorn HJ, Strobel MJ. Epidemiology of posterior cruciate ligament injuries. Arch Orthop Trauma Surg. 2003;123:186–91. https://doi.org/10.1007/s00402-002-0471-y.
38. Reider B. Medial collateral ligament injuries in athletes. Sports Med. 1996;21:147–56. https://doi.org/10.2165/00007256-199621020-00005.
39. Indelicato PA. Isolated medial collateral ligament injuries in the knee. J Am Acad Orthop Surg. 1995;3:9–14. https://doi.org/10.5435/00124635-199501000-00002.
40. Ngai SS, Tafur M, Chang EY, et al. Magnetic resonance imaging of ankle ligaments. Can Assoc Radiol J. 2016;67(1):60–8. https://doi.org/10.1016/j.carj.2015.09.002.
41. Park S, Lee S, Yoon J, et al. Finite element analysis of knee and ankle joint during gait based on motion analysis. Med Eng Phys. 2019;63:33–41. https://doi.org/10.1016/j.medengphy.2018.11.003.
42. Kedgley AE, Saw TH, Segal NA, et al. Predicting meniscal tear stability across knee-joint flexion using finite-element analysis. Knee Surg Sports Traumatol Arthrosc. 2019;27(1):206–14. https://doi.org/10.1007/s00167-018-5090-4.
43. Logerstedt DS, Ebert JR, MacLeod TD, et al. Effects of and response to mechanical loading on the knee. Sports Med. 2022;52(2):201–35. https://doi.org/10.1007/s40279-021-01579-7.
44. Liu H, Gong H, Chen P, et al. Biomechanical effects of typical lower limb movements of Chen-style Tai Chi on knee joint. Med Biol Eng Comput. 2023;61(11):3087–101. https://doi.org/10.1007/s11517-023-02906-y.
45. Demirtaş Y, Katı YA. A novel patella fracture fixation technique: finite element analysis. Arch Orthop Trauma Surg. 2023;143(8):5105–15. https://doi.org/10.1007/s00402-023-04910-1.
46. Cheng C, Zhang J, Jia J, et al. Influence of knee flexion on early femoral fracture healing: a combined analysis of musculoskeletal dynamics and finite elements. Comput Methods Programs Biomed. 2023;241: 107757. https://doi.org/10.1016/j.cmpb.2023.107757.
47. Pan M, Yin N, Du L, et al. A novel technique of a new cannulated screw for treatment of inferior pole patellar fractures: a finite element study. J Orthop Surg Res. 2023;18(1):795. https://doi.org/10.1186/s13018-023-04299-y.
48. Apostolopoulos V, Boháč P, Marcián P, et al. Biomechanical comparison of all-polyethylene total knee replacement and its metal-backed equivalent on periprosthetic tibia using the finite element method. J Orthop Surg Res. 2024;19(1):153. https://doi.org/10.1186/s13018-024-04631-0.
49. Zhang ZH, Qi YS, Wei BG, et al. Application strategy of finite element analysis in artificial knee arthroplasty. Front Bioeng Biotechnol. 2023;11:1127289. https://doi.org/10.3389/fbioe.2023.1127289.
50. Woiczinski M, Maas A, Grupp T, et al. Realitätsnahe Finite-Elemente-Simulation in der präklinischen Testung von Knie- und Hüftimplantaten [Realistic preclinical finite element simulation in knee and hip replacements]. Orthopade. 2020;49(12):1060–5. https://doi.org/10.1007/s00132-020-04025-0.
51. Baldwin MA, Clary CW, Fitzpatrick CK, et al. Dynamic finite element knee simulation for evaluation of knee replacement mechanics. J Biomech. 2012;45(3):474–83. https://doi.org/10.1016/j.jbiomech.2011.11.052.
52. Lampen N, Su H, Chan DD, et al. Finite element modeling with subject-specific mechanical properties to assess knee osteoarthritis initiation and progression. J Orthop Res. 2023;41(1):72–83. https://doi.org/10.1002/jor.25338.
53. Fukaya T, Mutsuzaki H, Aoyama T, et al. A simulation case study of knee joint compressive stress during the stance phase in severe knee osteoarthritis using finite element method. Medicina. 2021;57(6):550. https://doi.org/10.3390/medicina57060550.
54. Li L, Yang L, Zhang K, et al. Three-dimensional finite-element analysis of aggravating medial meniscus tears on knee osteoarthritis. J Orthop Translat. 2019;20:47–55. https://doi.org/10.1016/j.jot.2019.06.007.
55. Zhang X, Zhang M, Wang J, et al. Constructing digital model of knee joint and surrounding soft tissue surface by three-dimensional image registration technology. Chin J Tissue Eng Res. 2023;27(18):2814–9 (**In Chinese**).
56. Zhao Y, Zhang B, Feng X. Study on optimization value of knee prosthesis based on motion simulation. Zhongguo Gu Shang. 2023;31(03):22–5. https://doi.org/10.20085/j.cnki.issn1005-0205.230305.
57. Shu L, Yamamoto K, Yoshizaki R, et al. Multiscale finite element musculoskeletal model for intact knee dynamics. Comput Biol Med. 2022;141:105023. https://doi.org/10.1016/j.compbiomed.2021.105023.
58. Huang X. Sports injury modeling of the anterior cruciate ligament based on the intelligent finite element algorithm. J Healthc Eng. 2021;2021:3606863. https://doi.org/10.1155/2021/3606863.
59. He C, Li Y, Zhang Z, et al. Finite element analysis on biomechanical properties of knee ligaments under loading at different flexion angles. Chin J Sports Med. 2015;34(07):662–9.
60. Farshidfar SS, Cadman J, Deng D, et al. The effect of modelling parameters in the development and validation of knee joint models on ligament mechanics: a systematic review. PLoS ONE. 2022;17(1): e0262684. https://doi.org/10.1371/journal.pone.0262684.

Publisher's Note